Comput. Mater. Sci. **45** (2009) 744-750

Modeling the evolution of texture and grain shape in magnesium alloy AZ31 using crystal plasticity finite element method

Aruna Prakash[a,1], Sabine M. Weygand[b], Hermann Riedel[a]

[a]Fraunhofer Institute for Mechanics of Materials IWM, Woehlerstraße 11, 79108 Freiburg, Germany
[b]Forschungszentrum Karlsruhe GmbH, Institute for Materials Research II, 76344, Eggenstein Leopoldshafen, Germany

[1]Corresponding Author: Aruna Prakash<prakash@iwm.fraunhofer.de>

Abstract: The development of a strong basal texture upon processing has proven to be a major impediment in commercial applications of wrought magnesium alloys. The basal texture hampers further processing of the material, leading to high internal stresses and strain localization in the material. Under the framework of the crystal plasticity finite element method, a microstructural constitutive model for twinning has been developed to study the deformation characteristics of magnesium alloy AZ31. The concept of representative volume elements is used to identify internal stresses and strain localization in the material. Texture evolution and grain shape change are additional areas of interest in this work. The simulation results are compared with those from experiments to ascertain the trend of texture evolution.

1. Introduction

Magnesium, with its high strength-to-weight ratio and high impact strength, is a suitable candidate for use in the aerospace and automobile industry [1]. Most magnesium components, to date, are mainly produced as cast alloy components – e.g. mobile phones, gear box housings, gears and clutches etc., despite the fact that wrought alloy components exhibit a higher strength [2]. Wrought alloys of magnesium like AZ31 have been restricted in commercial usage due to low formability, which is mainly attributed to the HCP crystal structure and lack of sufficient glide systems at low temperatures. Additionally, the material develops a strong texture upon processing; for instance, during extrusion, the basal planes orient themselves parallel to the extrusion direction, and in rolling, the basal planes orient themselves in the rolling plane. This texture combined with the lack of sufficient slip systems leads to an inhomogeneity in deformation, ultimately leading to failure. By contrast, at higher temperatures, the processing becomes considerably easier, albeit with increased costs.

In this work, an attempt is made to study the deformation characteristics of magnesium using a Crystal Plasticity based Finite Element Model (CPFEM). Additionally, morphological and crystallographic textures are investigated. The CPFEM offers a few advantages in comparison to the well-known self-consistent (SC) texture models. The SC models [3-4] (e.g. VPSC [4]) fail to accurately predict grain shape change; the shape is always restricted to be an ellipsoid. This is obviously insufficient to describe complex morphologies such as *grain curling* in BCC wires [5]. Inter-granular and intra-granular stresses can be well predicted with CPFEM. In addition to the afore mentioned advantages, texture prediction with CPFEM is expected to be better than self-consistent models (texture in self consistent models is normally over-predicted [6]) thus, providing comparable results with the experiments.

2. Constitutive model

2.1 Crystal plasticity model

Grains in the polycrystalline aggregate are modeled within the framework of crystal plasticity [7,8]. The kinematics of deformation is based on Rice [9] and Hill & Rice [10]. In the original model, plastic deformation is assumed to be entirely due to dislocation movement (slip). In what follows, a few salient equations of the model are summarized.
Under the framework of large deformations, this model assumes a multiplicative decomposition of the deformation gradient F_{ij}.

$$F_{ij} = F^{*}_{ik} F^{p}_{kj} \,. \tag{1}$$

where, F^{p}_{ij} denotes plastic shear and F^{*}_{ij} accounts for elastic stretching and rotation of the lattice.

The rate of change of F^{p}_{ij} is related to the slipping rate $\dot{\gamma}^{(\alpha)}$ of the slip system α by

$$\dot{F}^{p}_{ik} F^{p^{-1}}_{kj} = \sum_{\alpha} \dot{\gamma}^{(\alpha)} s^{(\alpha)}_{i} m^{(\alpha)}_{j} \,, \tag{2}$$

where, $s^{(\alpha)}_{i}, m^{(\alpha)}_{j}$ are the slip direction and the slip plane normal, respectively.

It is convenient to define $s_i{}^{*(\alpha)}$, lying along the slip direction of the system α and $m_j{}^{*(\alpha)}$, normal to the slip plane, in the deformed configuration, by

$$\begin{aligned} s^{*(\alpha)}_{i} &= F^{*}_{ij} s^{(\alpha)}_{j}, \\ m^{*(\alpha)}_{j} &= m^{(\alpha)}_{j} F^{*-1}_{ij}. \end{aligned} \tag{3}$$

Based on the Schmid law, the shear rate $\dot{\gamma}^{(\alpha)}$ is determined by the resolved shear stress $\tau^{(\alpha)}$ on the slip system α in form of a power law,

$$\tau^{(\alpha)} = s_i^{*(\alpha)} \sigma_{ij} m_j^{*(\alpha)},$$
$$\dot{\gamma}^{(\alpha)} = \dot{a} \operatorname{sign} \tau^{(\alpha)} \left| \frac{\tau^{(\alpha)}}{g^{(\alpha)}} \right|^{1/n}, \quad (4)$$

where $\dot{a}$ denotes a reference shear rate, n denotes the material rate sensitivity and $g^{(\alpha)}$ describes the current strength of the system. The strain hardening is defined through a modified Voce hardening law:

$$\dot{g}^{(\alpha)} = \frac{d\hat{\tau}^{(\alpha)}}{d\Gamma} \sum_{\beta} h_{\alpha\beta} \dot{\gamma}^{(\beta)}, \quad (5)$$

where the diagonal elements of the hardening matrix $h_{\alpha\beta}$ describe self-hardening, and off-diagonal elements describe latent hardening. The hardening function $\hat{\tau}^{(\alpha)}$ is defined as:

$$\hat{\tau}^{\alpha} = \tau_0^{\alpha} + (\tau_1^{\alpha} + \theta_1^{\alpha}\Gamma)\left(1 - \exp\left(-\frac{\theta_0^{\alpha}\Gamma}{\tau_1^{\alpha}}\right)\right), \quad (6)$$

where τ_0^{α}, τ_1^{α}, θ_0^{α}, θ_1^{α} are the hardening parameters and Γ is the cumulative shear on all slip systems.

This entire constitutive structure has been implemented as a user material routine UMAT for *cubic symmetry* in the finite element code ABAQUS Standard® [11]. The UMAT has since been extended to describe deformation of HCP crystals [12] in addition to the Voce hardening law. Deformation in HCP materials depends strongly on the c/a ratio of the crystal. With a c/a ratio of 1.624, which is very close to the ideal ratio of 1.633, basal slip is the most preferred mechanism in magnesium. Two additional slip families are found, namely prismatic and pyramidal (<c+a>) slip. These slip systems are, however, less densely packed and hence require a higher critical resolved shear stress. In addition to dislocation glide, deformation may be accommodated by twinning, especially at low temperatures. Twinning in magnesium occurs usually on the {1 0 -1 2} <1 0 -1 1> *tensile twin* system. The geometry of the different deformation systems in Mg is schematically represented in fig 1.

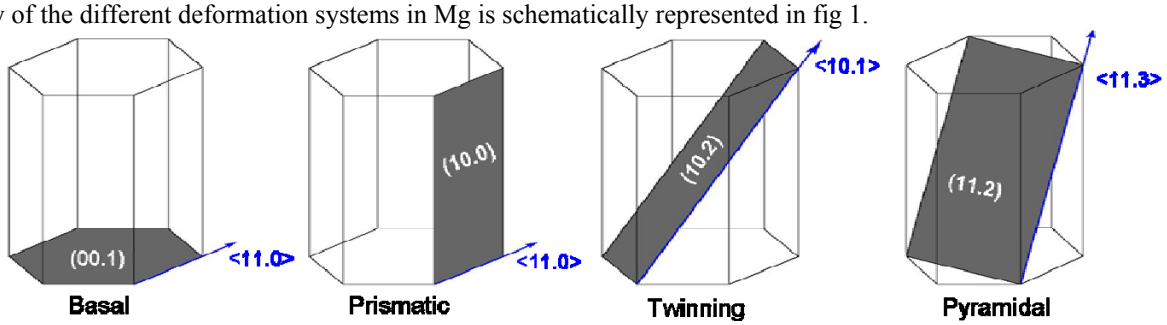

Fig 1: Deformation systems of Magnesium

2.2 Twinning

Twinning is essentially modeled as pseudo slip – shear along a twin system is allowed in only one direction – in order to account for the twin/anti-twin asymmetry [13]. The model for reorientation is based on the ideas of Van Houtte [14] and the predominant twin reorientation (PTR) scheme [15]. We define the evolution of the twin fraction by,

$$\dot{f}_{tw}^{(\alpha)} = \frac{\dot{\gamma}_{tw}^{(\alpha)}}{S}, \quad (7)$$

where $\dot{\gamma}_{tw}^{(\alpha)}$ is the shear on a particular twin system α and S is the characteristic shear of the twin family. With this twin fraction in hand, we define an "accumulated" twin fraction as,

$$f_{tw}^{acc} = \sum_{n}^{Steps} \sum_{\alpha}^{Ntw} \Delta f_{tw}^{(\alpha)}, \quad (8)$$

where the inner summation denotes summation over all twin systems and the outer summation denotes the accumulation over time. At any particular time increment, this accumulated twin fraction is compared with a threshold fraction F_T, which is a random number between 0 and 1. If the accumulated twin fraction is greater than the threshold fraction, reorientation is performed along the predominant twin system.

In the present finite element model, where a particular grain encompasses a number of elements, this twinning model completely reorients the crystal lattice of an integration point. The twinned part is not allowed to twin again, but may deform further by slip. This model, although very rudimentary, describes the basic properties of twinning activity in magnesium.

3. Finite element modeling

3.1 Representative volume element (RVE)

Although there has been a tremendous increase in computational power over the past few years, a complete macroscopic simulation using a crystal plasticity model is still extremely difficult. To circumvent this difficulty, one considers a unit cell built up of a sufficient number of grains, which is statistically *representative* of the material under consideration. Each grain is further

discretized fine enough to obtain a reasonable approximation of the intra-granular stresses along with the evolving microstructure and texture. A balance must thus be found between – a) having enough grains to make the unit cell representative, and b) having sufficient number of Gauss points per grain. To this end, we model the unit cell with 100 grains in a FE mesh of 20^3 linear brick elements; on an average a grain contains 640 integration points.

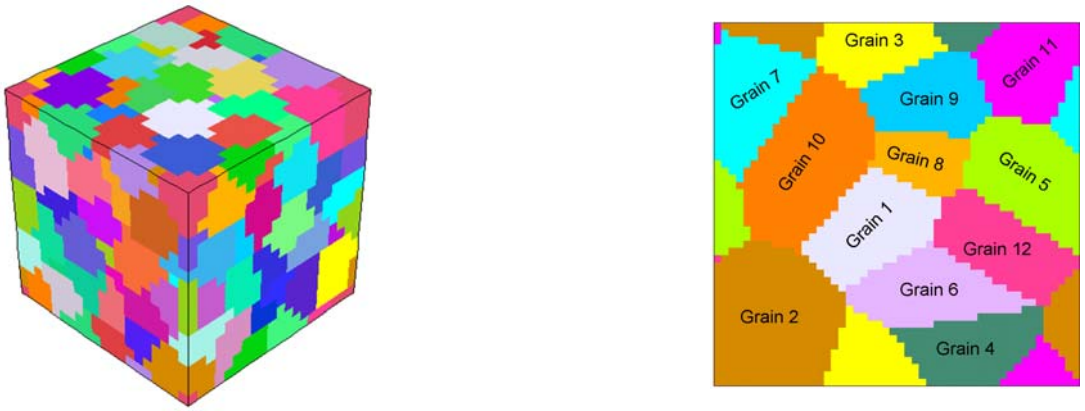

Fig 2: Input geometry used for FE simulations – a) 3D RVE with 100 grains, b) 2.5D model with 12 grains

The 3D RVE used in this work is shown in Fig 2a. For the purpose of obtaining information along the cross-section, a simpler model containing only one layer of 3D elements is used (Fig 2b). With such a model, a larger resolution per grain can be used and hence more details on a particular grain can be obtained. In what follows, this model is referred to as 2.5D. In addition to the periodic boundary conditions, the details of which are provided in the next section, this model is constrained to remain flat in its thickness. With such an approach, the results obtained can be approximated to that of a two dimensional analysis, although the model used is actually 3D. The 2.5D model contains 12 grains with 50^2 elements, giving an average of 1300 integration points per grain, which is twice the resolution of the complete 3D model. The 2.5D model can hence, be used to obtain finer details of deformation, although the unit cell cannot be regarded as representative.

3.2 Boundary conditions and material parameters

All the grains in the unit cell are given a random initial orientation to reflect a grey input texture. Initially, all integration points in a particular grain carry the same orientation. Plane strain compression conditions are used to achieve a thickness reduction of 40%. Periodic boundary conditions are used to minimize constraint effect. Essentially, two equivalent points a and b, located on opposite sides of the unit cell, are coupled with the macroscopic deformation gradient.

$$u_i^{\mathrm{b}} - u_i^{\mathrm{a}} = \overline{F}_{ij}\left(x_{j0}^{\mathrm{b}} - x_{j0}^{\mathrm{a}}\right) - \left(x_{i0}^{\mathrm{b}} - x_{i0}^{\mathrm{a}}\right), \tag{8}$$

where x^{a}_{i0}, x^{b}_{i0} indicate the position of a point pair in the non-deformed configuration.
The critical resolved shear stresses (CRSS) of the basal, twinning and prismatic systems are assumed to be in the ratio 1:1.25:1.5. The CRSS on the pyramidal system, when present, is assumed to be approximately 3 times that of the basal system. The hardening matrix in the Voce hardening law (eq. 5) is set to 1.0 for self hardening and slip-slip interaction. The latent hardening parameters for slip-twin and twin-twin interactions are set to 1.8 to account for the obstruction caused by twins to the movement of dislocations.

4. Simulation

4.1 Deformation characteristics

The 2.5D model was tested under plane strain compression with 40% thickness reduction. The model is constrained in the horizontal direction and compressed in the vertical direction. The rolling direction is perpendicular to the plane of paper. Results of two cases are presented, i) Absence of pyramidal slip, which represents the situation at low temperatures, and ii) Presence of pyramidal slip, which is characteristic for high temperature deformation. As can be inferred from fig 3a and fig 3b, the presence of pyramidal slip undoubtedly increases the uniformity of the deformation. The absence of pyramidal slip causes the deformation to proceed in an inhomogeneous fashion, with grain distortions – similar to the so called grain curling found in bcc wires [5,16] – occurring in the polycrystal. For the results shown in fig 3, a thickness reduction of just 27% could be achieved due to severe element distortions in the absence of pyramidal slip, whereas a complete 40% thickness reduction was achieved with pyramidal slip.

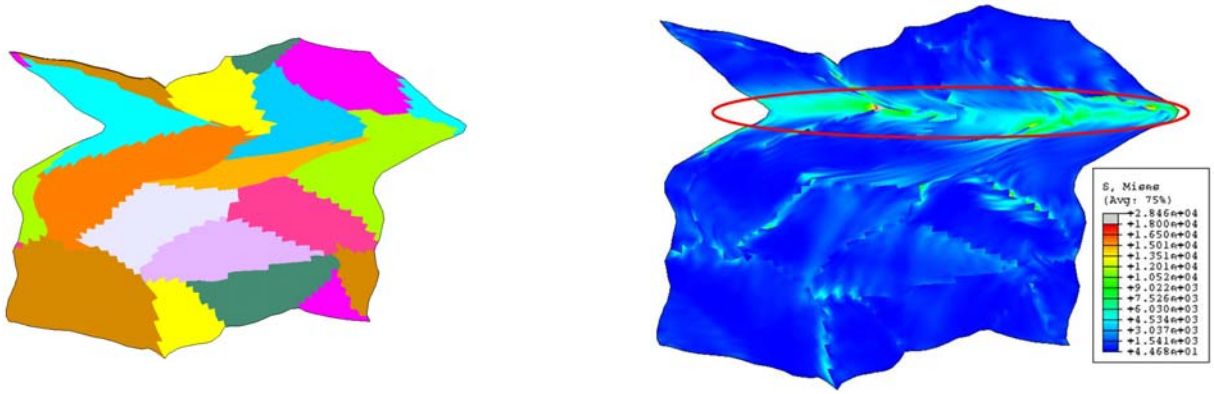

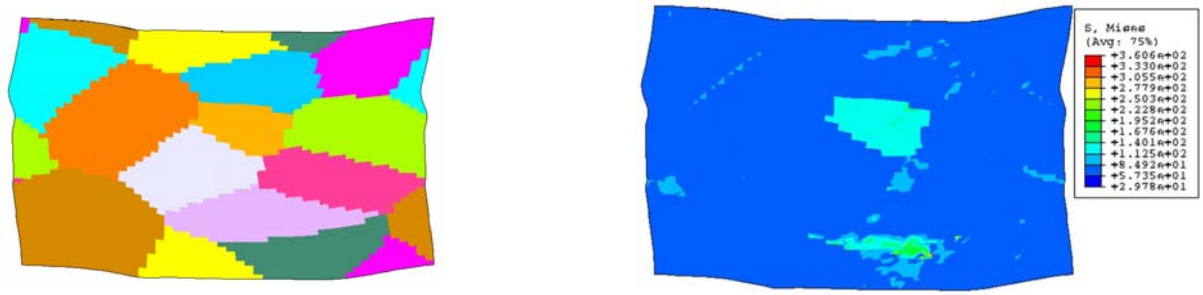

Fig 3: a) deformed configuration of microstructure without pyramidal slip after 27% thickness reduction; b) deformed configuration in the presence of pyramidal slip after 40% thickness reduction; c) stress in the polycrystal in the absence of pyramidal slip – regions of high stress coalesce to form a band (region marked by the red ellipse); d) stress in the polycrystal in the presence of pyramidal slip

The strong distortion of the grains in the absence of pyramidal slip is associated with high stress levels in the grain and stress concentrations at the grain boundaries (fig 3c). The regions of high stress levels in the grain coalesce to form a band which runs both inter-granular and trans-granular. Since the inhomogeneity in the absence of pyramidal slip is of particular interest, the subsequent sections present only results obtained in the absence of pyramidal slip. The reasons for this inhomogeneity are discussed in section 5.

4.2 Sub-graining

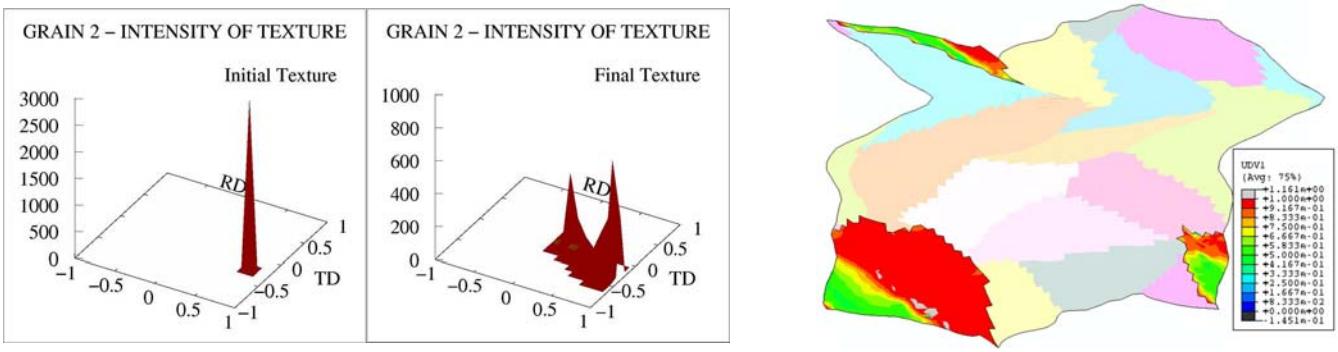

Fig 4: Sub-graining in the absence of pyramidal slip – a) Intensity of texture in the 0001 pole figure of grain 2; b) Contour plot of the direction-cosine of the angle between the compression direction and the c-axis

An additional phenomenon observed in the absence of pyramidal slip is sub-graining. This can be confirmed by looking into the texture evolution of grain 2, defined in fig 2b. Fig 4a shows the intensity of texture in the 0001 pole figure for grain 2. The initial texture of the grain can be represented as a single peak on the 0001 pole figure. After deformation, however, two distinct peaks are observed, which correspond to the nearly homogeneous areas of grain 2 (fig 4b).

4.3 Twinning

In order to obtain reasonable twinning reorientation activity, a different initial texture that facilitates twinning was assumed. The ratio of the CRSS was, however assumed to be the same. Fig 5 shows the twinning activity in the polycrystal in the absence of pyramidal slip. Prediction of twin lamellae is beyond the scope of the current model. The twinning activity, thus, needs to be viewed as a homogenization of twins in a particular grain. Although the implementation of twinning reorientation is an extremely rudimentary one, it suffices to capture the basic details of the twinning activity.

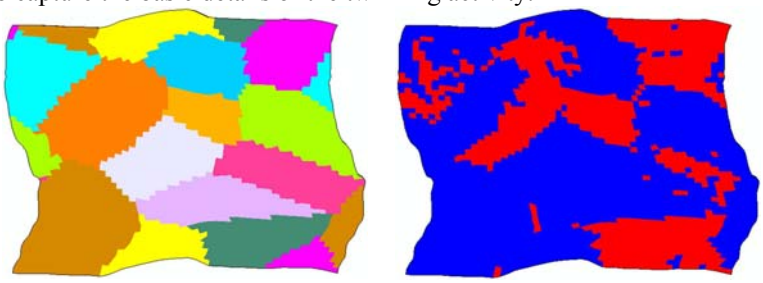

Fig 5: Twinning activity in the 2.5D model in the absence of pyramidal slip after approximately 25% thickness reduction: a) Deformed configuration after 25% thickness reduction b)Twinned elements marked with a light /red color

4.4 3-D RVE simulations

In order to ensure that the results obtained with the 2.5D model are qualitatively representative, 3D simulations with 100 grains are performed. The deformation characteristics in the absence of pyramidal slip are shown in fig 6. The deformation and stresses show the same characteristics as with the 2.5D simulations. Additionally, localized shear zones, at approximately 45°, can be observed in the RVE when viewed in the transverse direction. These shear zones might initiate recrystallization, which would be beneficial for the formability [17], but they can also cause fracture.

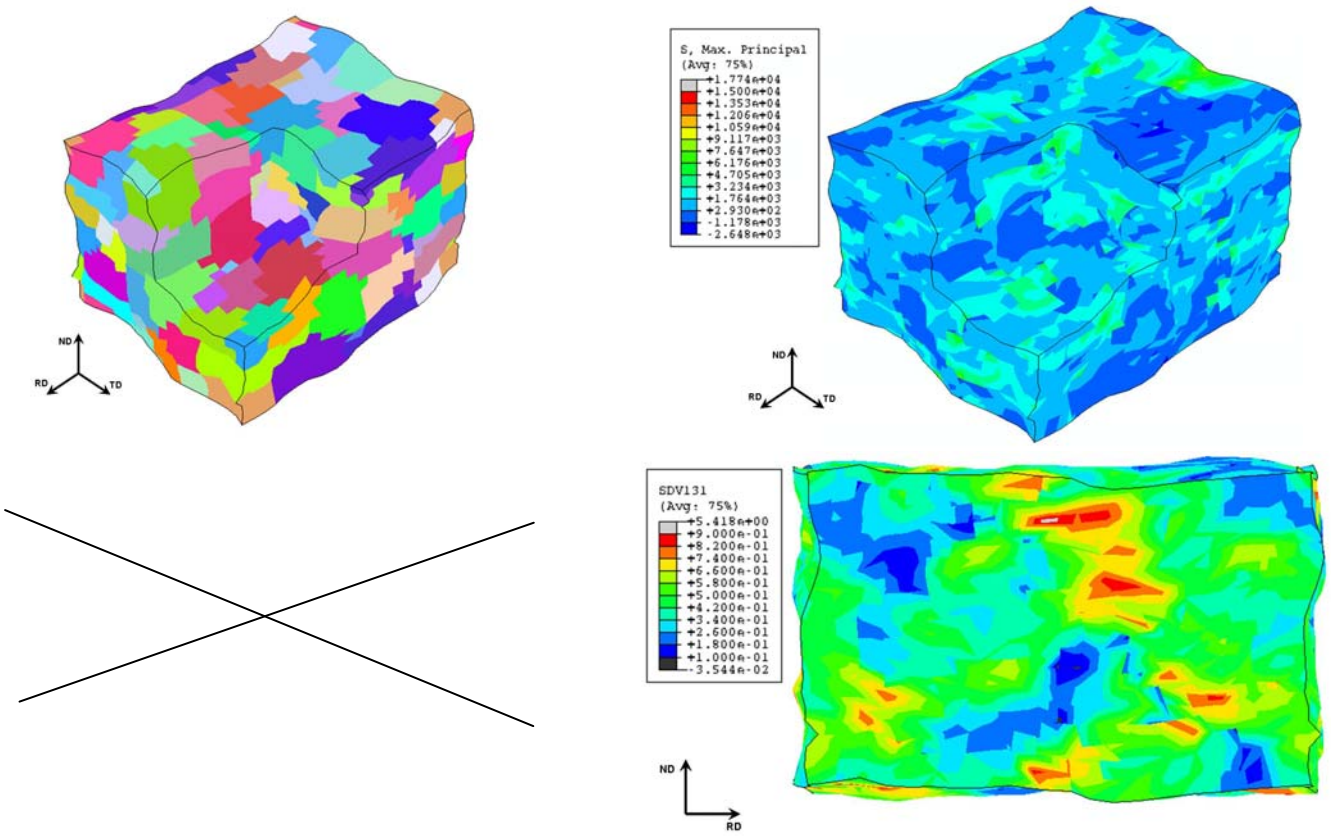

Fig 6: Deformation characteristics of the 3D model in the absence of pyramidal slip: a) Deformed configuration after 30% thickness reduction; b) Stress in the RVE; c) Accumulated plastic strain in the RVE viewed in transverse direction – note zones with high strain at approximately 45°

4.5 Crystallographic texture

Fig 7 shows the crystallographic texture obtained from the 3D simulation with 100 grains in the absence of pyramidal slip. For the purpose of experimental comparison, the final texture of a cast rolled sheet was used as reference. It must be added that due to lack of information on the thickness reduction of the cast rolled sheet, only the trend of texture evolution from the simulations was evaluated. Although the two textures do not match completely, it can be inferred that the trend of texture evolution from the simulation matches that of experiments very well.

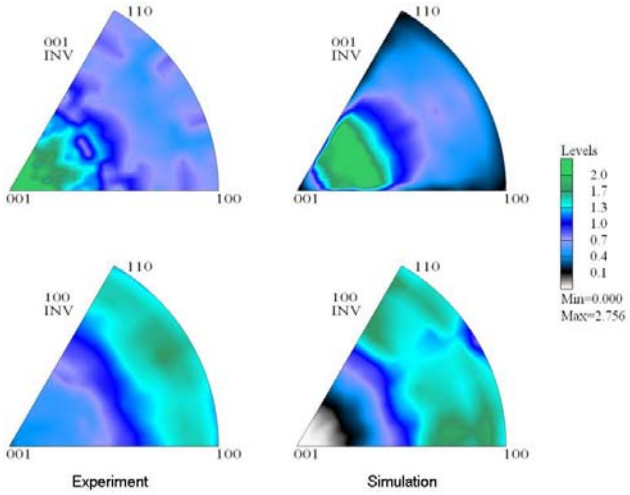

Fig 7: Crystallographic textures obtained from 3D simulations and a cast-rolled sheet; Top row – Inverse pole figures of the Normal direction; Bottom row – Inverse pole figures of the Rolling direction

5. Discussion

The inhomogeneity of deformation and the pronounced grain distortions in the absence of pyramidal slip can be better understood with the geometry of slip systems. Referring to fig 1, it can be inferred that the basal and prismatic slip share the same slip direction along the basal plane, commonly referred to as <a> slip. Hence, they cannot accommodate any deformation out of the basal plane. The out of plane deformation is accommodated to a certain extent by mechanical twinning, which is activated along the {1 0 -1 2} <1 0 -1 1> twinning system. This system, commonly known as tensile twinning, is activated only in the presence of a tensile component along the c-axis. Consequently, under plane strain compression, twinning in Mg can only be activated if the c-axis is oriented almost parallel to the rolling plane. Additionally, twinning is associated with a large and almost instantaneous

orientation change. This essentially reorients a crystal close to a basal orientation and further twinning activity will be restrained. Additional deformation is thus difficult to accommodate [18].

In the absence of pyramidal slip, one also observes grain distortions, similar to well-known grain curling phenomenon in bcc wires. Grains change their morphology and curl around each other to accommodate maximum deformation possible. Nevertheless, the desired thickness reduction of 40%, under plane strain compression, could not be achieved in the absence of pyramidal slip.

Pyramidal (<c+a>) slip accommodates slip in the out of plane direction and enhances deformation. A thickness reduction of around 65% could be easily achieved in the presence of pyramidal slip. The activation of pyramidal slip, however, requires a higher Peierls stress and is normally activated at temperatures above 200°C. Metal working of Mg alloys is hence strongly dependent on the initial texture and the temperature of processing.

6. Conclusions

a) Absence of pyramidal slip, which is usually thermally activated at temperatures above 200°C, is a major factor for the inhomogeneity of deformation during cold forming processes. Without pyramidal slip, morphological changes like grain curling and sub-graining could be observed under plane strain compression. Localized shear zones could also be observed in the absence of pyramidal slip.
b) At lower temperatures, twinning systems provide the deformation normal to the basal plane. However, since twinning is accompanied by a large orientation change, further deformation cannot be accommodated by twinning.
c) The 2.5D model with 12 grains was sufficient to capture the basic intricacies of the deformation process such as inhomogeneity, grain curling and sub-graining.
d) Presence of pyramidal slip eases the process of deformation substantially. This is due to the fact that it accommodates deformation in a direction normal to the basal plane.

6. Acknowledgements

The authors gratefully acknowledge the support of the German research foundation (DFG) under the framework of the magnesium priority program, SPP 1168 (Grant no. Rl 329). Additionally, the authors would like to thank Prof. R. Kawalla and C. Schmidt, Freiberg University of Mining and Technology, Freiberg, for providing the necessary data required for experimental comparison and our colleague Dr. O. Benevolenski in generating the unit cell using the software Palmyra.

7. References

[1] K.U. Kainer (Ed.): Proc. of the 6th international conf. magnesium alloys and their applications, Wiley-VCH, Weinheim, 2004

[2] B.M. Closset, J.F. Perey, C. Bonjour, P.A. Moos: Microstructure and properties of wrought magnesium alloys, *in: B.L. Mordike, K.U. Kainer (Eds.), Proc. Magnesium alloys and their applications*, Werkstoff-Informationsgesselschaft. Frankfurt (1998), 195

[3] A. Molinari, G.R. Canova and S. Ahzi: A self consistent approach of the large deformation polycrystal viscoplasticity, Acta metall., **35** (1987), 2983

[4] R.A. Lebensohn, C.N. Tomé: A self-consistent anisotropic approach for the simulation of plastic deformation and texture development of polycrystals: application to zirconium alloys, *Acta metal. Mater.*, **41** (1993), 2611

[5] W.F. Hosford: Microstructural changes during deformation of [011] fiber textured metals, *Trans. AIME* **230** (1964), 12

[6] R. Kawalla, C. Schmidt, H. Riedel, A. Prakash: Experimental and numerical investigation of texture development during hot rolling of magnesium alloys, *in: K.U. Kainer (Ed.) Proc. of the 7th intl. conf. on magnesium alloys and their applications*, Dresden, 2006, 1048

[7] R.J. Asaro: Crystal Plasticity, *Journal of Applied Mech.,* **50** (1983), 921

[8] R.J. Asaro: Micromechanics of Crystals and Polycrystals, *Adv. Appl. Mech.*, **23** (1983)**,** 1

[9] J.R. Rice: Inelastic constitutive relations for solids, *J. Mech Phys. Solids*, **19** (1971), 433

[10] R. Hill, J.R. Rice: Constitutive analysis of elastic-plastic crystals at arbitrary strain, *J. Mech. Phys. Solids*, **20** (1972), 401

[11] Y.G. Huang: *A User-material Subroutine Incorporating Single Crystal Plasticity in the ABAQUS Finite Element Program*, Harvard Univ. (1991), Rep. MECH-178

[12] S.M. Schlögl: Micromechanical modeling of the deformation behavior of gamma titanium aluminides, *Ph.D thesis* (1997), Univ. of Leoben, Austria

[13] S.M. Schlögl, F.D. Fischer, The role of slip and twinning in the deformation behaviour of polysynthetically twinned crystals of TiAl: a micromechanical model, *Phil. Mag. A* , **75** (1997), 621

[14] P. Van Houtte: Simulation of rolling and shear texture of brass, *Acta metallurgica*, **26** (1978), 591

[15] C.N. Tomé, R.A. Lebensohn, U.F. Kocks: A model for texture development dominated by deformation twinning, *Acta metallurgica,* **39** (1991), 2667

[16] J. Očenášek, M. Rodriguez Ripoll, S. M. Weygand, H. Riedel: Multi-grain finite element model for studying the wire drawing process, *Computational Materials Science*, **39** (2007), 23

[17] S.E. Ion, F.J. Humphreys, S.H. White: Dynamic recrystallization and the development of microstructure during the high temperature deformation of magnesium, *Acta metallurgica*, **30** (1982), 1909

[18] G. Gottstein, T. Al Samman: Texture development in pure Mg and Mg alloy AZ31, Mat. Sci. Forum, **495-497** (2005), 623